Journal of Alloys and Compounds 711 (2017) 335–341

Contents lists available at ScienceDirect

Journal of Alloys and Compounds

journal homepage: http://www.elsevier.com/locate/jalcom

The effect of ligand chain length on the optical properties of alloyed core-shell InPZnS/ZnS quantum dots

Yemliha Altıntas [a], Mohammad Younis Talpur [b], Evren Mutlugun [b, *]

[a] Abdullah Gül University, Department of Materials Science and Nanotechnology Engineering, 38080, Kayseri, Turkey
[b] Abdullah Gül University, Department of Electrical-Electronics Engineering, 38080, Kayseri, Turkey

ARTICLE INFO

Article history:
Received 20 September 2016
Received in revised form
8 February 2017
Accepted 28 March 2017
Available online 29 March 2017

Keywords:
Cd-free quantum dots
Alloyed core/shell
Photoluminescence
Optical properties
Organic ligands

ABSTRACT

In this work, we demonstrate the effect of organic ligands on the optical properties of alloyed core-shell InPZnS/ZnS quantum dots (QDs). We have systematically studied the synthesis and characterization of InPZnS/ZnS QDs using short and long chain length ligands i.e., butyric (C4), hexanoic (C6), octanoic (C8), dodecanoic (C12), myristic (C14), palmitic (C16) and stearic acids (C18), respectively. This study achieved more than 85% quantum yield with 43 nm full-width-half maximum value, using dodecanoic acid as the capping ligand. The properties of the QDs with short and long chain length ligands have been analyzed using UV–Vis absorption spectrophotometer, steady state and time resolved photoluminescence spectrometer, X-ray diffraction, Zeta sizer, transmission electron microscopy and energy dispersive X-ray spectroscopy.

1. Introduction

Colloidal quantum dots (QDs) have been extensively used in optoelectronics due to their superior optical and electronic properties. Their high quantum efficiency stemming from the good carrier confinement by coating of a wider band gap shell material, tunability in their peak emission wavelength by controlling their size and composition and ease in surface functionalization by engineering their ligands have made colloidal quantum dots available for versatile applications in optoelectronics, i.e., light emitting platforms [1] and solar cells [2]; and in biotechnology, i.e., for sensing [3,4] and diagnosis [5].

One of the most important aspects of the QDs is their surface, which makes the inorganic core material active for potential applications. The ligands passivates the core from the dangling bonds, prevent agglomeration, enhance the photoluminescence, provide a barrier against the environment and also play a critical role to restrict the nucleation and growth stages in the synthesis [6]. In charge driven applications, such as QD electroluminescent devices [7], or architectures based on charge collection such as solar cells [8], the organic ligands have an important function in determining the efficiency of the overall working device controlling the charge injection. Therefore, in the first place, it is important to identify the effect of the ligand on the optical properties of the colloidal quantum dots. Also the excitonic engineering within colloidal QDs is critically important for optoelectronic applications [9]. Lately, non-radiative energy transfer (NRET) has been shown to be an efficient tool for advanced optoelectronics including lighting and solar energy harvesting devices. In that aspect, there is a critical role of interparticle distance, thus the ligand chain length to study the excitonic interactions for QD based devices. In this work, we have used short and long chain organic ligands for the optimization of the QD optical properties, as organic materials are active excitonic components of the material systems as reported in the literature [10]. Organic ligands consist of large bulky molecules that act as insulating barrier between QDs, possibly hindering charge transfer [11]. It has also been shown in the literature that the interparticle distance can lead to enhanced performance in spectrally pure quantum dot based light emitting diodes [12].

In an effort for the synthesis of environmentally friendly particles, we have focused or attention to InP based QDs which holds great potential due to their non-heavy metal nature. In recent years, there has been an increased effort to achieve high efficiency; narrow bandwidth InP based QDs [13,14]. Alloying core InP material with the Zn has recently been shown in multiple reports to provide high quantum yield particles [15,16]. Battaglia et al. reported the

* Corresponding author.
E-mail address: evren.mutlugun@agu.edu.tr (E. Mutlugun).

http://dx.doi.org/10.1016/j.jallcom.2017.03.326
0925-8388/

long carbon chain ligands for the synthesis of InP core quantum dots [17]. To the best of our knowledge, there is no information available in the literature focusing on the extensive investigation of the effect of ligands in the optical properties of the InP based QD system.

In this work we report an extensive study of the synthesis of alloyed core/shell InPZnS/ZnS QDs using butyric (C_4), hexanoic (C_6), octanoic (C_8), dodecanoic (C_{12}), myristic (C_{14}), palmitic (C_{16}) and stearic (C_{18}) acid ligands systematically for synthesis of highly efficient, color tunable InP based QDs.

2. Experimental procedure

2.1. Synthesis of colloidal quantum dots

The following chemicals have been purchased from Sigma Aldrich and used without further purification: Indium acetate (99.99%), butyric acid (99+%), hexanoic acid (98+%), octanoic acid (98+%), dodecanoic acid (98%), myristic acid (99%), palmitic acid (95%), stearic acid (grade I), oleic acid, 1-dodecanethiol (98%), zinc stearate (purum), tris(trimethylsilyl)phosphine (95%), 1-octadecene (90%), hexane, acetone (99.5%) and methanol (99.8%).

For the synthesis of InPZnS/ZnS alloyed core-shell QDs, we follow the modified recipe in the literature [14,18] which has been outlined in our previous work [15]. In a typical synthesis 0.1 mmol of indium acetate and 0.3 mmol of the associated long and short carbon chain ligand (i.e., butyric acid, hexanoic acid, octanoic acid as the short chain length; and dodecanoic acid, myristic acid, palmitic acid, stearic acid as the long chain length ligand) were mixed in 6 mL of octadecene in a three-neck flask, and kept under the vacuum for 1 h at 100 °C. Flushing the system with Argon gas, the temperature is raised to 120 °C and kept until getting a clear solution. The flask was cooled down to room temperature and 0.1 mmol of zinc stearate and 0.025 mmol of dodecanethiol were mixed with the Indium-ligand complex, and the mixture was heated at 220 °C under Ar gas flow. At the elevated temperature, 0.1 mmol of tris(trimethylsilyl)phosphine in 1 mL of octadecene was quickly introduced to the system and upon waiting 30 s, the temperature was raised to 285 °C. (for the synthesis with short chain length ligands, the tris(trimethylsilyl) phosphine injection has been carried out at 200 °C and the temperature was raised to 230 °C after injection) After waiting for 10 min, the alloyed core growth process has been established. After cooling the flask, 0.2 mmol of zinc stearate was added to the reaction flask and the temperature was raised to 230 °C under Ar flow. After 3 h of reaction, 0.4 mmol of 1-dodecanethiol in 1 ml of octadecene was injected to the reaction flask dropwise (with a rate of 10 ml/h) and reaction was established at that temperature and kept at that temperature for 1 h. Upon completion of the synthesis, the reaction was cooled down to room temperature, and the QDs were precipitated twice, using acetone-methanol extraction by centrifuge (10 min at 5000 rpm). The precipitated particles have been dissolved in fresh solvent of hexane or chloroform.

2.2. Calculation of the quantum yield

The quantum efficiency of the synthesized QDs was measured using Rhodamine 6G as a reference dye, by comparing the integrated emission intensity of the reference dye and the QD as discussed in our previous work [15]. The excitation wavelength have been determined using the absorbance spectrum of both QDs and the reference dye (the excitation wavelength is determined by the intersection of the absorbance spectrum in the range 460–490 nm, where the absorbance level is in the range of 0.1 to prevent re-absorbtion.) The quantum yield has been calculated using the following Equation.

$$QE_{QD} = QE_{Ref} \times \left(I_{QD}/I_{Ref}\right) \times \left(A_{Ref}/A_{QD}\right) \times \left(n_{QD}/n_{Ref}\right)^2 \quad (1)$$

Here the QE is the quantum yield, I is the integrated fluorescence intensity, A stands for absorbance (the term A_{Ref}/A_{QD} is taken as unity in our case due to intersection of the spectra), and n is the refractive index of the solvent used.

2.3. Characterization methods

Quantum dot photoluminescence measurements have been recorded using Cary Eclipse and absorption spectra is collected using Thermo Genesys 10S. The time correlated single photon counting measurements have been carried out using Fluo Time 200 system, equipped with 375 nm pulsed laser diode. X-ray diffraction experiments were performed using PANalytical: X'pert Pro MPD and transmission electron microscopy images were taken with FEI - Model: Tecnai G2 F30 (with EDAX). The quantum dot size information and distribution have further been obtained using Malvern-Zeta sizer.

3. Results and discussions

Fig. 1(a and b) and 2 (a and b) shows the absorbance and photoluminescence (PL) spectra for the quantum dots synthesized with long chain length ligands of dodecanoic acid, myristic aid, palmitic acid, stearic acid and short chain length ligands of butyric acid, hexanoic acid and octanoic acid. We observe that the PL emission peak wavelength varies in the range of 490–515 nm and the full width at half maximum value (FWHM) is in an increasing trend with the increase in the chain length. We clearly observe that the short chain length ligands do not provide enough stabilization to the quantum dot of interest; therefore the quantum efficiency (QE) is much suppressed as compared with the long chain length ligands. However, we observe that the dodecanoic acid with C12 possess the maximum quantum yield and further increasing the chain length of the ligands to C14, C16 and C18 causes the reduction of the QE of the synthesized nanocrystals. The enhancement of the QE with increasing the chain length of the ligand to some extent and reduction with the further increasing the ligand length is in a similar trend with the study of Ouyang et al. [19], which shows the evaluation of the quantum yield of CdS quantum dots with changing the carbon chain length. Fig. 3 shows the change in the QE and PL emission peak wavelength vs. the type of the ligand used. The QE depends on the type of ligands with short and long hydrocarbons along with functional organic group (carboxylic group). Tables 1 and 2 present the quantum yield, the peak emission wavelength, full width half maximum and the 1st excitonic peak position of the quantum dots with the corresponding ligand. Considering the change of the QE with FWHM, in general QE increases with decreasing the FWHM. This is an expected observation since FWHM is related with the degree of the carrier confinement within the nanocrystals. As the carriers are more confined in the core, this enhances the PL quantum yield and provides better size distribution. We have investigated that increasing the ligand chain length from C4, C6, C8, C12, C14, C16 and C18; the QE was calculated as 27, 49, 48, 86, 85, 75 and 70% with FWHM determined as 48, 45, 45, 43, 45, 46 and 52 nm, respectively. Here it is worth noting that our achievement of quantum yields above 85% with 43 nm of FWHM value is one of the best ever reported value for such InP based colloidal nanocrystals. This behavior indicates that C12 capped QDs give rise to high QE as compared to shorter or longer chain

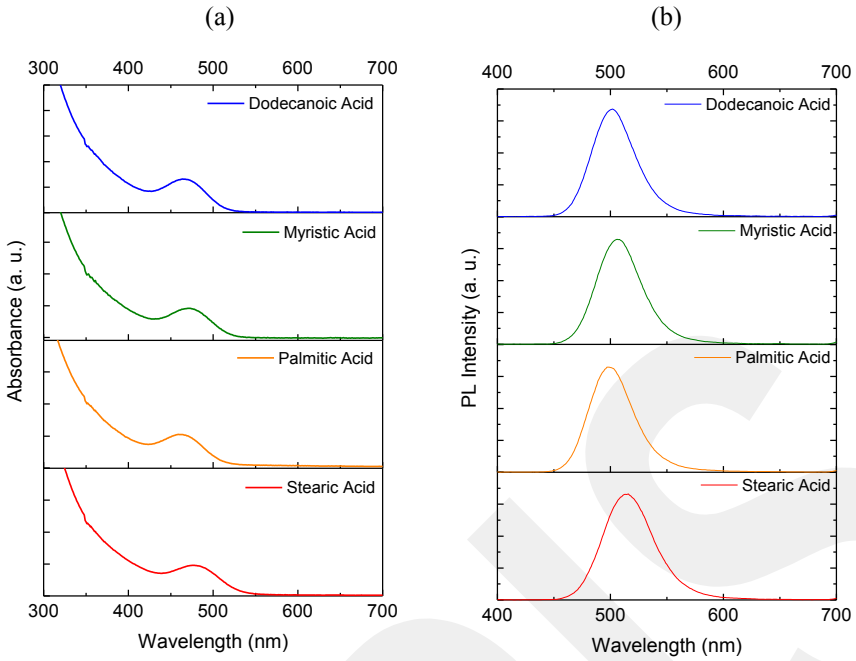

Fig. 1. (a) Absorbance and (b) photoluminescence spectra for the quantum dots synthesized with long chain fatty acid ligands.

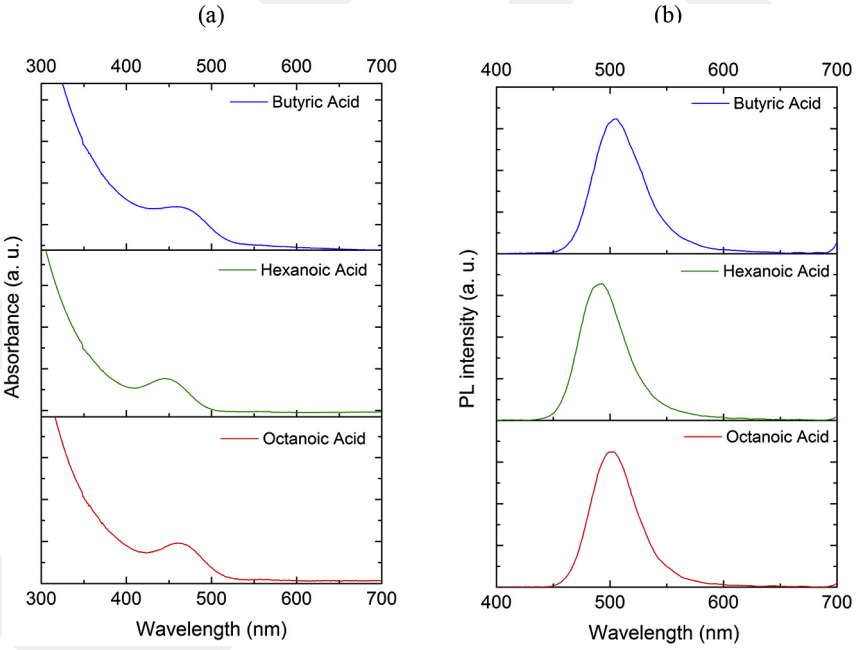

Fig. 2. (a) Absorbance and (b) photoluminescence spectra for the quantum dots synthesized with short chain fatty acid ligands.

ligands, which is due to a better surface passivation influenced by an optimal ligand density. In addition, QE depends on the surface quality of the QDs mainly, based on the type of the ligands. Short chain ligands (C4, C6 and C8) has been proposed to possess lowest QE as compared to the long chain ligands (C12, C14 and C18), which is possibly due to the equilibrium of the adsorption-desorption, which can lead to a non optimal passivation of QD's surface trap states. The observation of the decrease of the QE when using longer ligand length is attributed to the larger steric hindrance of the bulky molecules within atoms of the molecule. Longer ligand chain length (i.e., C16 and C18) possess more steric hindrance in the atoms of the molecule (hydrogen-carbon and carbon-carbon atoms) as compared to C12 along with the organic functional group that steric hindrance for these bulky molecules prevents complete passivation, therefore possibly creating non-radiative de-excitation pathways. In this regard, further increasing the chain length beyond C12, the QE was decreased. The steric hindrance by long hydrocarbons limits the interaction between indium and $(TMS)_3P$, preventing the optimal reaction. On the other hand, the short chain organic ligands are observed to possess less QE due to incomplete surface passivation of the QDs and can lead more non-radiative de-excitation behavior.

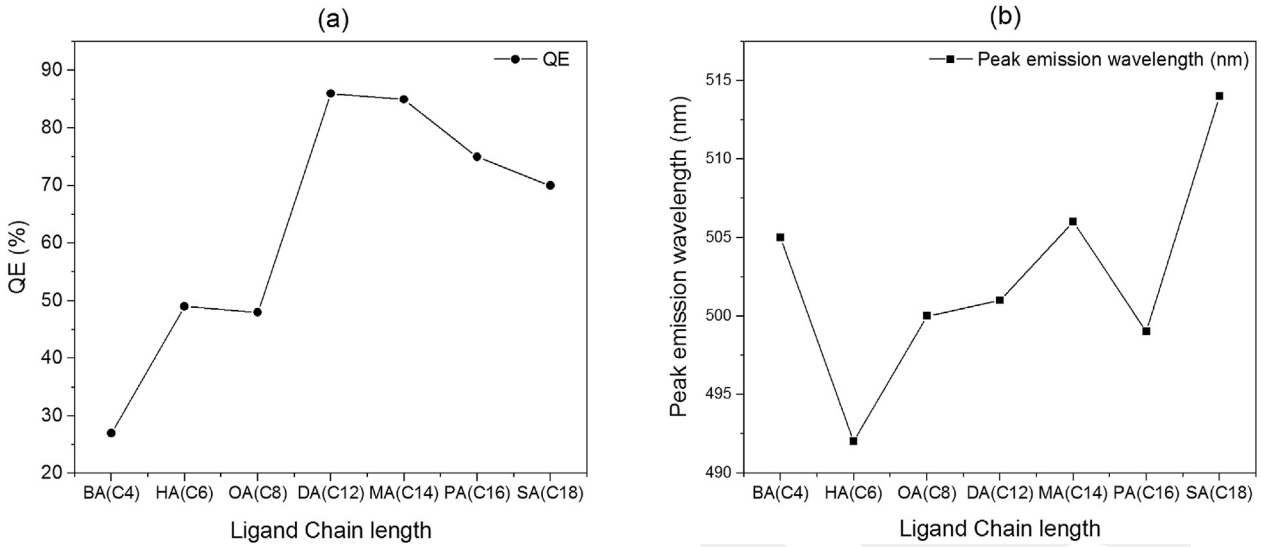

Fig. 3. a) Quantum efficiency (QE) and b) peak emission wavelength of InPZnS/ZnS QDs with respect to the ligand used.

Table 1
Comparison of optical properties of QDs with long chain length ligands.

Organic Ligand	QE (%)	PL λ_{max} (nm)	FWHM (nm)	1st excitonic peak (nm)	Stokes' shift (nm)	Stokes' shift (meV)
Dodecanoic Acid (C12)	86	501	43	466	35	186
Myristic Acid (C14)	85	506	45	471	35	182
Palmitic Acid (C16)	75	499	46	462	37	199
Stearic Acid (C18)	70	514	52	477	37	187

Furthermore, as can be seen in Tables 1 and 2, The QE and Stokes Shift have a correlation between them. Basically, the general trend in our study is that, a decrease in the QE is accompanied by an increase of Stokes' Shift. The QE (C4, C6 and C8) of the short chain ligands is less than long chain ligands. From this perspective short chain ligands have been shown to possess higher Stokes' Shift as compared with the ones with longer chain ligands.

We further compared the ligands of C18 of stearic acid and oleic acid. As given in Table 3, the use of double bond C ligand has not shown to have a significant effect on the optical properties of the synthesized particles.

Having an overview of the effect of the ligands on the optical properties of the synthesized quantum dots, we have further analyzed the long and short chain ligand quantum dots. For the analysis, we have used C6- hexanoic acid (HA) and C18- stearic acid (SA). Tables 4 and 5 presents the energy dispersive X-ray measurements of the particles with HA and SA ligands. EDX measurements shows that by weight, the QDs with stearic acid ligands are composed of 30.48% In, 5.90% P, 59.51% Zn, and 4.10% S whereas QDs with hexanoic acid ligands are composed of 28.16% In, 12.56% P, 38.89% Zn, and 20.39% S. We attribute the high efficiency of the C18 as compared to C6, to the higher zinc content of the synthesized particles, which would suppress the dangling bonds in the resulting alloyed core structure. In addition, we also observe that the In:P ratio is higher in the case of C18 as compared to C6 having less photoluminescence QE, which is in agreement with our previous work [15].

Fig. 4a shows the photoluminescence excitation spectra comparison for QDs synthesized using HA and SA. We have found out that the above the band edge, approaching the UV, the long chain length particles possess higher photoluminescence excitation intensity as compared to the nanocrystals with short chain length. In order to reveal the emission kinetics, we have investigated the lifetime of the HA and SA quantum dots by using the pulsed laser at

Table 2
Comparison of optical properties of QDs with short chain length ligands.

Organic Ligand	QE (%)	PL λ_{max} (nm)	FWHM (nm)	1st excitonic peak (nm)	Stokes' shift (nm)	Stokes' shift (meV)
Butryric Acid (C4)	27	505	48	465	40	211
Hexanoic Acid (C6)	49	492	45	446	46	260
Octanoic Acid (C8)	48	500	45	461	39	210

Table 3
Comparison of optical properties of QDs with single and double bond C18 ligands.

Used acid	QE (%)	PL λ_{max} (nm)	FWHM (nm)	1^{st} excitonic peak (nm)
Stearic Acid (C18)	70	514	52	477
Oleic Acid (C18)	70	511	48	473

Table 4
Energy dispersive X-ray analysis for QDs with hexanoic acid (C6) ligands.

Element	Weight %	Atomic %	Uncert. %
In(L)	28.16	13.03	2.69
P(K)	12.56	21.55	1.44
Zn(K)	38.89	31.62	2.90
S(K)	20.39	33.80	1.69

Table 5
Energy dispersive X-ray analysis for QDs with stearic acid (C18) ligands.

Element	Weight %	Atomic %	Uncert. %
In(L)	30.48	17.76	1.87
P(K)	5.90	12.75	0.85
Zn(K)	59.51	60.91	2.50
S(K)	4.10	8.55	0.71

375 nm. The photoluminescence lifetime decays are depicted in Fig. 4b and curves have been fit using 3-exponentials. The corresponding coefficients, lifetime components and average and intensity weighted lifetimes are presented in Table 6. The lifetime components of the QDs with HA, namely τ_1, τ_2 and τ_3 are given as 90.12 ns, 32.93 ns and 4.87 ns; whereas the lifetime components of the QDs with SA is found as 78.24 ns, 35.67 ns, and 5.05 ns. As investigated further, the contribution of the longest lifetime component τ_1 is 39.0% for the HA, whereas 48.1% for the SA; for τ_2 it is calculated as 41.7% for the HA and 40.6% for the SA; and the contribution of the τ_3 is found as 19.2% for the HA and 11.2% for the SA capped particles respectively. As the calculated quantum yields have been calculated as 49% and 70% for the HA and SA capped particles; we attribute the increase in the contribution of the short lifetime component of the HA as compared with SA to the non-radiative decay channels of the QD emitter. Therefore we can further assume that the longer the chain length, the more is the suppression of the non-radiative channels for the quantum dot emitter. The calculated amplitude weighted lifetime is 49.87 ns for the HA, and 52.73 ns for the SA capped particles. Fig. 4c presents the photograph of the emitters under the same UV exposure, showing the more saturated color for the SA capped particles.

We have also compared the physical sizes of the HA and SA capped quantum dots. Our results have been presented in Fig. 5 along with the transmission electron microscopy images. Since

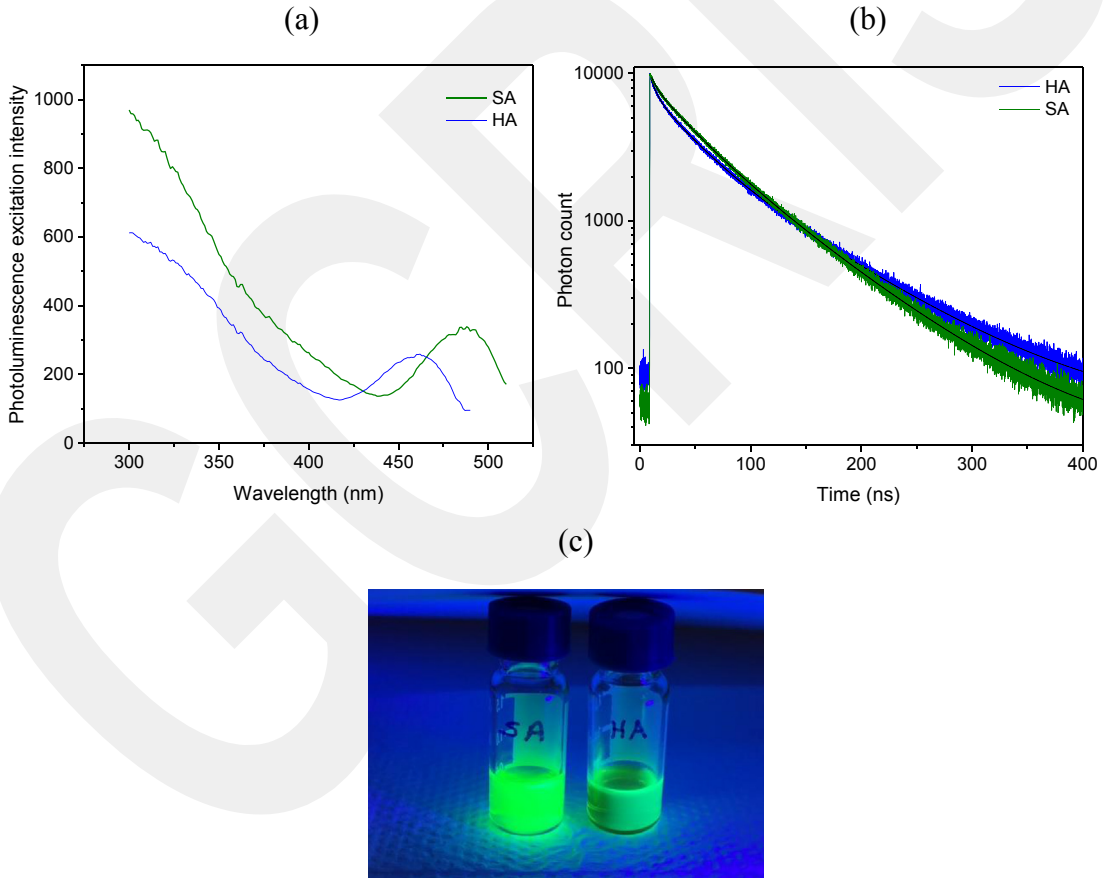

Fig. 4. (a) Photoluminescence excitation spectra, (b) time resolved photoluminescence decay curves QDs with hexanoic acid (HA) and stearic acid (SA) ligands (c) Photo of the QDs under UV illumination.

Table 6
Amplitudes, lifetime components and average and intensity weighted lifetimes of quantum dots with hexanoic acid (HA) and stearic acid (SA) ligands, extracted from time resolved photoluminescence measurements.

	A_1	τ_1 (ns)	A_2	τ_2 (ns)	A_3	τ_3 (ns)	$\tau_{average}$ (ns) (intensity)	$\tau_{average}$ (ns) (amplitude)
HA	3594.9 ± 23.6	90.12 ± 0.44	3843.1 ± 56.4	32.93 ± 0.48	1768 ± 181	4.87 ± 0.65	72.76	49.87
SA	4507.6 ± 28	78.24 ± 0.36	3806.9 ± 55.8	35.67 ± 0.52	1050 ± 181	5.05 ± 1.15	65.74	52.73

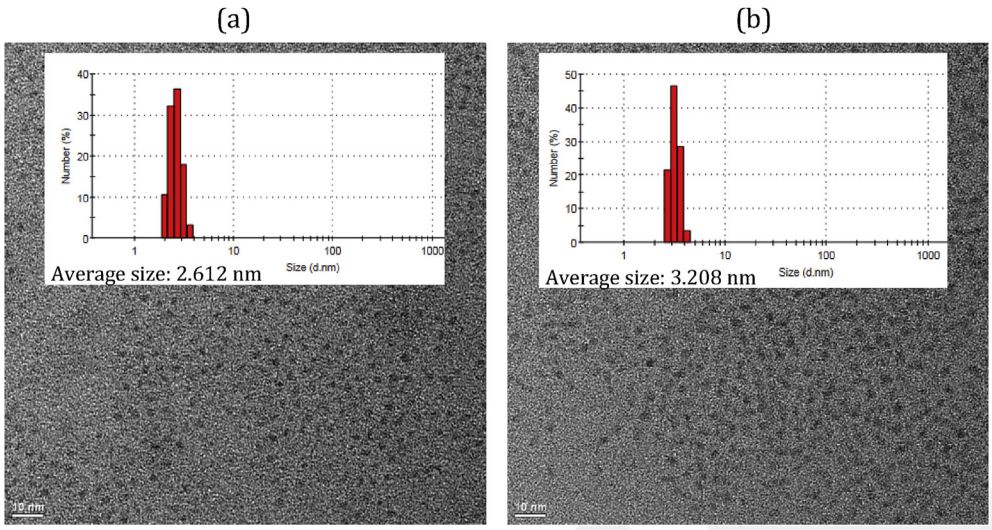

Fig. 5. Transmission electron microscopy image for QDs with (a) hexanoic acid (b) stearic acid ligands. Insets show the dynamic light scattering measurement histograms for both QDs.

the resolution was not high to make a clear size comparison, we have analyzed the size distribution using the Zeta sizer and the size histograms have been included as inset to the graph. Our results indicate that the average size achieved for the HA and SA capped QDs is given as 2.612 nm and 3.208 nm, respectively. The difference in sizes of particles is attributed directly to the change in the chain length for both particles and in agreement in order of magnitude when compared with the single carbon chain. For the investigation of the crystal structure we have carried out the X-ray diffraction measurement. The peaks observed at ≈ 27°, 45°, and 54° is attributed to the cubic zinc blende structure, corresponding to the (111), (220), (311) planes. The peaks have been found to be more pronounced for the quantum dots with stearic acid (see Fig. 6).

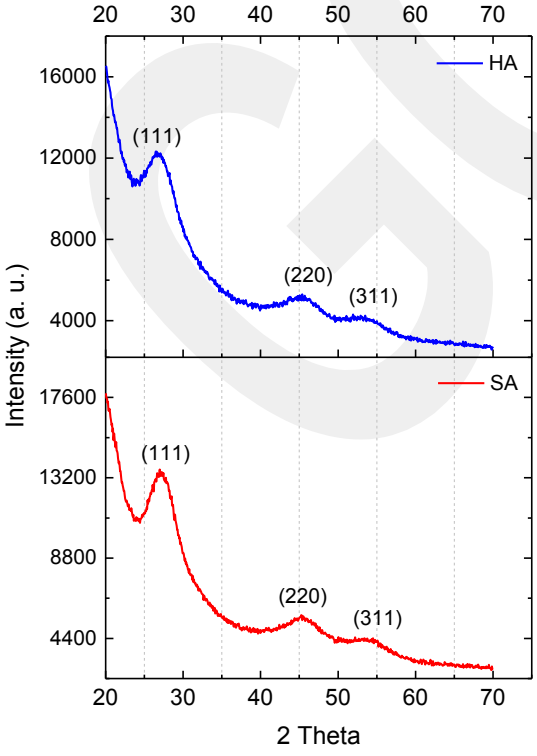

Fig. 6. X-ray diffraction pattern of QDs with (a) hexanoic acid (b) stearic acid ligands.

4. Conclusions

In conclusion, we have made a systematic study of the effect of the organic ligands on the optical properties of the alloyed core-shell InPZnS/ZnS QDs. In that respect we have used butyric (C4), hexanoic (C6), octanoic (C8), dodecanoic (C12), myristic (C14), palmitic (C16) and stearic acids (C18) as the capping agents. We have clearly observed from the data that using of C12-dodecanoic acid as the capping organic ligand for the synthesis of alloyed-core/shell InPZnS/ZnS QDs possess the highest quantum efficiency of 86% with 43 nm FWHM value. We have further made in depth investigation of the PL emission kinetics of the QDs for a better understanding of the correlation of the optical properties with the chain length of the ligands. We have characterized long and short ligand chain length QDs with time resolved photoluminescence spectrometer, resulting in QDs with short (hexanoic acid) and long chain length ligand (stearic acid) having lifetime of 49.87 ns and 52.73 ns respectively. This study could provide further insight for the application driven design of the colloidal quantum dot emitters.

Acknowledgements

The authors would like to acknowledge support from The Scientific and Technological Research Council of Turkey TUBITAK under project no's 114E107, 5140079. The authors thank research group of Prof. Hilmi Volkan Demir at Bilkent University for their support in time resolved photoluminescence measurements. EM acknowledges BAGEP 2014 Award. MYT acknowledges TUBITAK BIDEB 2221 Fellowship.

References

[1] H.V. Demir, S. Nizamoglu, T. Erdem, E. Mutlugun, N. Gaponik, A. Eychmüller, Quantum dot integrated LEDs using photonic and excitonic color conversion, Nano Today 6 (6) (2011) 632–647.
[2] P.V. Kamat, Quantum dot solar cells. Semiconductor nanocrystals as light harvesters, J. Phys. Chem. C 112 (2008) 18737–18753.
[3] M. Bruchez, M. Moronne, P. Gin, S. Weiss, A.P. Alivisatos, Semiconductor nanocrystals as fluorescent biological labels, Science 281 (1998) 2013–2016.

[4] Y. Zhang, T.H. Wang, Quantum dot enabled molecular sensing and diagnostics, Theranostics 2 (2012) 631–654.
[5] T.M. Samir, M.M.H. Mansour, S.C. Kazmierczak, H.M.E. Azzazy, Quantum dots: heralding a brighter future for clinical diagnostics, Nanomedicine 7 (2012) 1755–1769.
[6] M.A. Boles, D. Ling, T. Hyeon, D.V. Talapin, The surface science of nanocrystals, Nat. Mater. 15 (2016) 141–153.
[7] P.O. Anikeeva, J.E. Halper, M.G. Bawendi, V. Bulovic, Quantum dot light-emitting devices with electroluminescence tunable over the entire visible spectrum, Nano Lett. 9 (7) (2009) 2532–2536.
[8] J. Tang, K.W. Kemp, S. Hoogland, K.S. Jeong, H. Liu, L. Levina, M. Furukawa, X. Wang, R. Debnath, D. Cha, K.W. Chou, A. Fischer, A. Amassian, J.B. Asbury, E.H. Sargent, Colloidal-quantum-dot photovoltaics using atomic-ligand passivation, Nat. Mater. 10 (2011) 765–771.
[9] B. Guzelturk, P.L.H. Martinez, Q. Zhang, Q. Xlong, H. Sun, X.W. Sun, A.O. Govorov, H.V. Demir, Excitonic of semiconductor quantum dots and wires for lighting and displays, Laser Photonics Rev. 8 (2014) 73–93.
[10] S.K. Saikin, A. Eisfeld, S. Valleau, A.A. Guzik, Photonics meets excitonics: natural and artificial molecular aggregates, Nanophotonics 2 (2013) 21–38.
[11] D.V. Talapin, J.-S. Lee, M.V. Kovalenko, E.V. Shevchenko, Prospects of colloidal nanocrystals for electronic and optoelectronic applications, Chem. Rev. 110 (2010) 389–458.
[12] E. Mutlugun, B. Guzelturk, A.P. Abiyasa, Y. Gao, X.W. Sun, H.V. Demir, Colloidal quantum dot light-emitting diodes employing phosphorescent small organic molecules as efficient exciton harvesters, J. Phys. Chem. Lett. 5 (2014) 2802–2807.
[13] E. Ryu, S. Kim, E. Jang, S. Jun, H. Jang, B. Kim, S.W. Kim, Step-wise synthesis of InP/ZnS core-shell quantum dots and the role of zinc acetate, Chem. Mater. 21 (2009) 573–575.
[14] T. Kim, S.W. Kim, M. Kang, S.-W. Kim, Large-scale synthesis of InPZnS alloy quantum dots with dodecanethiol as a composition controller, J. Phys. Chem. Lett. 3 (2012) 214–218.
[15] Y. Altıntas, M.Y. Talpur, M. Unlu, E. Mutlugun, Highly efficient Cd-Free alloyed core/shell quantum dots with optimized precursor concentrations, J. Phys. Chem. C 120 (14) (2016) 7885–7892.
[16] F. Pietra, L.D. Trizio, A.W. Hoekstra, N. Renaud, M. Prato, F.C. Grozema, P.J. Baesjou, R. Koole, L. Manna, A.J. Houtepen, Tuning the lattice parameter of InxZnyP for highly luminescent lattice-matched core/shell quantum dots, ACS Nano 10 (4) (2016) 4754–4762.
[17] D. Battaglia, X. Peng, Formation of high quality InP and InAs nanocrystals in a noncoordinating solvent, Nano Lett. 2 (9) (2002) 1027–1030.
[18] L. Li, P. Reiss, One-pot synthesis of highly luminescent InP/ZnS nanocrystals without precursor injection, J. Am. Chem. Soc. 130 (2008) 11588–11589.
[19] J. Ouyang, J. Kuijper, S. Brot, D. Kingston, X. Wu, D.M. Leek, M.Z. Hu, J.A. Ripmeester, K. Yu, Photoluminescent colloidal CdS nanocrystals with high quality via noninjection one-pot synthesis in 1-octadecene, J. Phys. Chem. C 113 (18) (2009) 7579–7593.